RESEARCH ARTICLE

PROTEINS WILEY

A hyperthermophilic protein G variant engineered via directed evolution prevents the formation of toxic SOD1 oligomers

Bar Dagan[1] | Ofek Oren[2] | Victor Banerjee[1,3] | Ran Taube[2] | Niv Papo[1,3]

[1]Avram and Stella Goldstein-Goren Department of Biotechnology Engineering, Faculty of Engineering, Ben-Gurion University of the Negev, Beer-Sheva, Israel

[2]The Shraga Segal Department of Microbiology, Immunology and Genetics, Faculty of Health Sciences, Ben-Gurion University of the Negev, Beer-Sheva, Israel

[3]The National Institute for Biotechnology in the Negev, Beer-Sheva, Israel

Correspondence
Niv Papo, Department of Biotechnology Engineering and the National Institute of Biotechnology, Ben-Gurion University of the Negev, P.O. Box 653, Beer-Sheva 84105, Israel.
Email: papo@bgu.ac.il

Funding information
European Research Council (ERC), Grant/Award Number: 336041; Israel Science Foundation (ISF), Grant/Award Number: 615/14

Abstract

Amyotrophic lateral sclerosis (ALS) is a fatal neurodegenerative disorder characterized by selective death of motor neurons in the brainstem, motor cortex, and spinal cord, leading to muscle atrophy and eventually to death. It is currently held that various oligomerization-inducing mutations in superoxide dismutase 1 (SOD1), an amyloid-forming protein, may be implicated in the familial form of this fast-progressing highly lethal neurodegenerative disease. A possible therapeutic approach could therefore lie in developing inhibitors to SOD1 mutants. By screening a focused mutagenesis library, mutated randomly in specific "stability patch" positions of the B1 domain of protein G (HTB1), we previously identified low affinity inhibitors of aggregation of SOD1$_{G93A}$ and SOD1$_{G85R}$ mutants. Herein, with the aim to generate a more potent inhibitor with higher affinity to SOD1 mutants, we employed an unbiased, random mutagenesis approach covering the entire sequence space of HTB1 to optimize as yet undefined positions for improved interactions with SOD1. Using affinity maturation screens in yeast, we identified a variant, which we designated HTB1$_{M3}$, that bound strongly to SOD1 misfolded mutants but not to wild-type SOD1. In-vitro aggregation assays indicated that in the presence of HTB1$_{M3}$ misfolded SOD1 assembled into oligomeric species that were not toxic to NSC-34 neuronal cells. In addition, when NSC-34 cells were exposed to misfolded SOD1 mutants, either soluble or preaggregated, in the presence of HTB1$_{M3}$, this inhibitor prevented the prion-like propagation of SOD1 from one neuronal cell to another by blocking the penetration of SOD1 into the neuronal cells.

KEYWORDS

affinity maturation, amyloid aggregation, amyloid infectivity, amyotrophic lateral sclerosis, misfolded SOD1

1 | INTRODUCTION

Neurodegenerative diseases are incurable diseases that are characterized by the formation of amyloid aggregates and the gradual death of neurons. One such disease is amyotrophic lateral sclerosis (ALS), a fatal disorder characterized by the selective death of motor neurons in the brainstem, motor cortex, and spinal cord, leading to muscle atrophy and death. Disease progression has been linked to protein inclusions in the motor neurons of patients with ALS—both sporadic and familial ALS (fALS),[1,2] where fALS comprises 10% of all ALS cases. Mutations in the Cu/Zn-superoxide dismutase (SOD1) gene are implicated in 20% of fALS cases and 5% sporadic cases[1,2]; these mutations destabilize the native protein and lead to its aggregation and accumulation into inclusions, indicating a strong connection between disease progression and SOD1 misfolding and aggregation.[3-5] Evidence for the role of SOD1 in the development of ALS was drawn from studies in mice showing that symptoms similar to those found in ALS patients were produced by overexpression of SOD1 mutants

(SOD1$_M$) or even by overexpression of SOD1$_{WT}$.[6] These studies showed that high levels of misfolded SOD1 and SOD1 aggregates were present in motor neurons of transgenic mice expressing either SOD1$_M$ or SOD1$_{WT}$.[6]

The aggregation pathway of SOD1 (both wild type and mutant) is initiated by the loss of single copper and zinc ions located on each of the two subunits of the homodimeric SOD1 molecule. This step is followed by protein misfolding and the formation of different SOD1 oligomers, some of which evolve into mature amyloid fibrils, finally producing a heterogeneous mix of prefibrillar oligomers and mature amyloid fibrils. Although the aggregation of SOD1 is a hallmark of ALS, it is unclear whether misfolded monomeric SOD1, misfolded oligomers on the fibrillization pathway (on-pathway oligomers), misfolded off-pathway oligomers, or fully formed misfolded amyloid fibrils are responsible for the toxic effect of SOD1 in ALS.[7-10]

Another hallmark property of SOD1 (and indeed of amyloid-forming proteins in general) is its potential to exhibit a prion-like behavior, which contributes to its high toxicity and in the case of misfolded SOD1 correlates with the fast progression of the disease.[11] Both misfolded SOD1$_M$ and SOD1$_{WT}$ exhibit prion-like behavior, propagating spatiotemporally from single or multiple focal points, consisting of one or more neurons, through the brain stem, motor cortex, and spinal cord.[12-16] For the prion-like spread of SOD1 from cell to cell to take place, misfolded SOD1 must first be excreted by the cells into the extracellular space, and extracellular SOD1 has indeed been detected in the cerebrospinal fluid (CSF) of both sporadic ALS and fALS patients.[17] Similarly, it has been shown that SOD1 is secreted by cultured neuronal cells expressing the mutant or wild-type form of the protein.[18,19] Subsequent uptake of misfolded SOD1 by neighboring neurons has been shown to be highly efficient, taking place via the macropinocytosis endocytic pathway,[20] and once inside the cells, misfolded SOD1 seeds misfolding and aggregation of endogenous SOD1 in the infected neurons, eventually resulting in apoptosis. These findings suggest that the spread of misfolded SOD1 from neuron to neuron is indirect, taking place via secretion of the misfolded SOD1 into the CSF and its subsequent uptake by naïve neurons.

The above observations are enabling the design of new strategies to treat fALS and sporadic ALS[21,22]; among them are approaches to target both intracellular and extracellular misfolded SOD1 and thereby to prevent SOD1 aggregation and toxicity. For example, active immunization with the SOD1 exposed dimer interface (SEDI) antigenic peptide delayed disease onset and extended survival in two mouse models of ALS, one overexpressing SOD1$_{G37A}$ and the other overexpressing SOD1$_{G93A}$.[23] Similarly, intracerebroventricular infusion of monoclonal antibodies that target misfolded forms of extracellular SOD1 extended the survival of SOD1$_{G93A}$ transgenic mice.[22] In yet another study, adeno-associated virus serotype 9 (AAV9) encoding an shRNA-mediated suppression of SOD1$_{G93A}$ expression reduced the levels of mutant SOD1 in the spinal cords of SOD1$_{G93A}$ transgenic mice and extended their survival.[24] Nonetheless, these approaches and others, although potentially promising, were either unable to significantly delay the rapid progression of the disease or failed at clinical trials.[25,26]

Our approach to targeting misfolded SOD1 and preventing its neuron internalization and aggregation into toxic species rests on exploiting an inhibitor based on the hyperthermophilic variant of the B1 domain of protein G (HTB1) as a protein scaffold, since HTB1 has previously been shown to have the potential for producing variants that bind amyloids, albeit with low affinity.[27] Based on this approach, our group previously developed an inhibitor that we designated HTB1$_M$, which was evolved by screening a focused mutagenesis library, mutated in "stability patch" positions.[28] HTB1$_M$ was shown to inhibit the aggregation of the two structurally and functionally dissimilar fALS-linked SOD1 mutants SOD1$_{G93A}$ and SOD1$_{G85R}$, but with low affinity.[28] We now think it likely that the low affinity of HTB1$_M$ for SOD1 derived from the assumption that the binding site of HTB1 to SOD1 would be found in the selected stability patches. In keeping with this notion, we posit that HTB1$_M$ binds to SOD1 via residues that were not chosen for mutation in our previous study and that the HTB1$_M$-based inhibitor can therefore be further optimized. Thus, as we report here, to generate a more potent inhibitor with higher affinity to SOD1 mutants, we employed a random mutagenesis approach to mutate all the residues of the protein (including residues that had not been mutated in the previous study). Using affinity maturation screens in yeast, we identified HTB1$_{M3}$, which bound to SOD1 mutants G85R and G93A with high affinity and specificity and inhibited their aggregation in vitro (but did not bind to SOD1$_{WT}$). We also found that addition of HTB1$_{M3}$ to the culture medium of NSC-34 neuronal cells conferred a dual protective action: it caused misfolded SOD1 to organize into prefibrillar oligomers in such a way that they were not toxic to the cells, and it prevented misfolded or aggregated SOD1 from penetrating inside the neuronal cells in a prion-like manner.

2 | MATERIALS AND METHODS

2.1 | SOD1 aggregation and inhibition of aggregation by HTB1$_{M3}$

SOD1 mutants (SOD1$_{G93A}$ and SOD1$_{G85R}$) were incubated under aggregation-inducing conditions (37 °C, 600 RPM orbital shaking) at 50 μM in 200 μL of 20 mM Na$^+$/phosphate buffer, pH 7.4, 100 mM NaCl, 1 mM tris(2-carboxyethyl)phosphine (TCEP) and 1 mM ethylenediaminetetraacetic acid (EDTA) for 96 hours in 1.5-mL Eppendorf tubes. Prior to incubation, all samples were filtered through 0.22-μm pore size hydrophilic PVDF membrane filters (Millipore, Burlington, Massachusetts) to remove aggregates. HTB1$_{M3}$ was prepared separately in the same buffer, and added to the samples in final concentrations of 1 to 25 μM. Every 24 hours, 20 μL of the resulting SOD1 solution was taken out and stored at 4 °C until the end of the experiment. After 96 hours, 180 μL of thioflavin T (ThT) solution containing 50 μM ThT, 50 mM Na$^+$/phosphate buffer, pH 7.4, and 100 mM NaCl in deionized water was added to the 20-μL aliquots of the SOD1 solution samples, and after 30 minutes of incubation at room temperature, ThT fluorescence was measured at an excitation wavelength of 445 nm and an emission wavelength at 485 nm by

using an Infinite M1000 (Tecan, Männedorf, Switzerland) plate reader. All experiments where performed in triplicate, and statistical analyses were performed using ANOVA and Dunnett's post-test.

2.2 | Cell cultures and viability assays

NSC-34 cells were cultured in DMEM complete medium comprising Dulbecco's modified eagle medium (DMEM) high glucose, with 10% fetal bovine serum (FBS), 1% Pen Strep solution and 1% L-glutamine. The cells were maintained in T-75 cell culture flasks and subcultured every 2 to 3 days at a confluency of ~100%, keeping 1/4 to 1/8 of the cells and discarding the rest. To detach the cells from the flask, 3 mL of trypsin-EDTA solution B was used. To determine cell viability, an XTT-based cell viability assay was used according to the manufacturer's protocol (Biological Industries, Beit-Haemek, Israel).

2.3 | SOD1$_{G93A}$ cell penetration assays

SOD1$_{G93A}$ was conjugated to Alexafluor-647 by NHS-ester chemistry. Briefly, AlexaFluor-647, 100 μg, was suspended in 10 μL of DMF, and the suspension was added to 1 mg of SOD1$_{G93A}$ in Na$^+$/phosphate buffer, pH 7.6, and 100 mM NaCl. After incubating the reaction mixture for 40 minutes at room temperature, the conjugated protein was eluted on a PD-10 desalting column (GE Healthcare, Chicago, Illinois), and the eluate was collected in 0.5-mL fractions. Fractions containing high concentrations of protein, measured with a NanoDrop spectrophotometer, were combined and concentrated in a Vivaspin 5 kDa cutoff (0.5 mL tubes; GE Healthcare) to a final concentration of 150 μM. Fluorescently labeled proteins were aliquoted and stored at −20 °C until use. Purified HTB1$_{M3}$ was conjugated to Dylight-488 by applying a similar protocol, but with 50 μg of Dylight-488 and 0.5 mg of HTB1$_{M3}$, and concentrated in a Vivaspin 3 kDa cutoff (0.5 mL tubes; GE Healthcare) to a final concentration of 55 μM.

After conjugation, SOD1$_{G93A}$ was allowed to aggregate under aggregation-inducing conditions identical to those in the aggregation experiments described above. After 48 hours of aggregation, protein samples were dialyzed overnight in PBS at 4 °C to remove TCEP and EDTA prior to addition to the NSC-34 cells. To test for SOD1$_{G93A}$ penetration, 1×10^4 NSC-34 cells were plated in each well of a 96-well flat-bottom cell culture plate. After 4 hours, the culture medium was replaced with DMEM complete medium containing 0.5 μM SOD1$_{G93A}$ in either aggregated (48 hours, 37 °C, 600 RPM orbital shaking) or nonaggregated form. Before the medium was changed, HTB1$_{M3}$ was added to the medium containing SOD1$_{G93A}$. After 16 hours, the medium was aspirated, cells were trypsinized with trypsin-EDTA solution B and transferred to a U-bottom 96-well plate for washing. Cells were washed three times with 200 μL of PBS by pelleting the cells at 150 g for 5 minutes and gently flipping the plate to remove supernatant. After three washes, cells were resuspended in 100 μL of PBS and analyzed by FACS (Accuri C6 flow cytometer, BD Biosciences, San Jose, California) for geometric mean fluorescence. Triplicates of each sample were used for statistical analysis. For microscopy experiments, NSC-34 cells were plated at

2×10^4 cells per well in a μ-Slide 8-well (Ibidi, Martinsried, Germany) and treated with SOD1$_{G93A}$ and HTB1$_{M3}$ in the same manner as above. Instead of removing the cells from the plate, they were washed three times with PBS while adhering to the plate and imaged after adding 1 μg/mL of Hoechst dye. Representative results from experiments conducted in triplicate are presented below.

2.4 | Reagents

All enzymes and enzyme buffers were obtained from New England Biolabs (Ipswich, Massachusetts). Oligonucleotides were purchased from Integrated DNA Technologies (San Jose, California). *Saccharomyces cerevisiae* EBY100 strain and the yeast surface display (YSD) plasmid (pCTCON) were kind gifts from the laboratory of Dane Wittrup (MIT, Cambridge, Massachusetts). All media and their components for bacteria and yeast growth were purchased from Sigma (St. Louis, Missouri), as was ThT. Chicken anti-c-Myc antibody (ab19233) was purchased from Abcam (Cambridge, United Kingdom), and goat anti chicken IgY (sc3730) was purchased from Santa Cruz Biotechnology (Dallas, Texas). FITC-conjugated NeutrAvidin was purchased from Invitrogen (Carlsbad, California). The NSC-34 cell line was a generous gift from Dr. Adrian Israelson, Ben-Gurion University of the Negev, Beer-Sheva, Israel. All media and medium additives for NSC-34 cell cultures were purchased from Biological Industries (Kibbutz Beit-Haemek, Israel). AlexaFluor-647 and Dylight-488 NHS-esters were purchased from Thermo Fischer Scientific (Waltham, Massachusetts). A11 polyclonal antibody (AHB0052) was obtained from Thermo Fisher Scientific.

3 | RESULTS

3.1 | HTB1$_M$ mutagenesis and screening for binding to SOD1$_{G93A}$ and SOD1$_{G85R}$

In our previous study, we used a combination of computational/semi-rational (mapping protein surfaces predisposed to HTB1 intermolecular interactions) and combinatorial (library screening by yeast surface display) approaches to engineer a novel protein, HTB1$_M$, that specifically binds misfolded SOD1$_{G93A}$ and SOD1$_{G85R}$ and inhibits the formation of cytotoxic SOD1 aggregates both intracellularly and extracellularly.[28] The current study builds on that work but addresses one of its inherent limitations, namely, that the semi-rational approach, by its very nature, ignores amino acid positions not chosen for mutation. However, these positions may include mutations that can affect binding affinity, either through direct contacts, which in the absence of structural information are difficult to predict, or through allosteric effects.[29] The other shortcomings that we address here are: the low affinity of HTB1$_M$ for SOD1$_{G93A}$ and SOD1$_{G85R}$, the lack of studies on the ability of HTB1$_M$ to prevent the transfer of misfolded SOD1 from cell to cell, and the lack of characterization of the SOD1 oligomeric species formed in the presence of HTB1$_M$. In the current study, we used a random mutagenesis approach, which does not impose any bias in terms of residues or amino acid

composition. To further reduce any undesirable bias, we first constructed two individual libraries, each by using a different method of mutagenesis, and then sorted the two libraries independently against both SOD1$_{G93A}$ and SOD1$_{G85R}$ by repeatedly reducing the SOD1 concentration and collecting only the variants showing high binding affinity relative to their expression on the yeast cells (Figures S1 and S2). In addition, the individual variants isolated from the sorted libraries were tested independently for binding to SOD1$_{G93A}$ and SOD1$_{G85R}$ (Figure 1A). This selection process yielded HTB1$_{M4}$, which had the strongest binding affinity (normalized to expression) found to date to both targets (Figure 1A-C). Thereafter, we monitored the enrichment of the frequency of specific clones by individually sequencing all libraries after sorting against both SOD1$_{G85R}$ and SOD1$_{G93A}$, yielding HTB1$_{M3}$, which showed the highest frequency in the high-affinity sorting gate (Figure 1B). A more comprehensive description of the mutagenesis and screening process is given in Supporting Information. The two selected HTB1 variants were expressed in *Escherichia coli* BL21 and purified by affinity chromatography (Figure S3; the full purification process is described in Supporting Information). During the refolding process of the purified protein variants, HTB1$_{M4}$ precipitated in each of the sequential buffer changing and concentration steps. It appears that the protein tends to self-aggregate at high concentrations when folded and therefore is not as good a candidate for a therapeutic as HTB1$_{M3}$, which did not precipitate. Therefore, we chose to move forward to the activity and cell assays with HTB1$_{M3}$ alone.

Surface plasmon resonance (SPR) was used to determine the binding affinity of purified HTB1$_{M3}$ to the SOD1 mutants. Binding constants were calculated as K_D = 305 ± 55 nM for SOD1$_{G93A}$ and K_D = 912 ± 109 nM for SOD1$_{G85R}$, and as expected, no binding was detected for SOD1$_{WT}$ (Figure S4).

3.2 │ HTB1$_{M3}$ inhibits the aggregation of SOD1$_{G93A}$ and SOD1$_{G85R}$

ThT fluorescence was used to monitor SOD1$_{G93A}$ and SOD1$_{G85R}$ amyloid aggregates in vitro. To test for inhibition of aggregation by HTB1$_{M3}$, the SOD1 mutants were incubated for 96 hours under aggregation-inducing conditions, in the presence or absence of HTB1$_{M3}$, and ThT fluorescence was followed. In the presence of HTB1$_{M3}$, the aggregation of the SOD1 mutants was inhibited in a manner that was dependent on the molar ratio of HTB1$_{M3}$ to SOD1 mutant. Inhibition of aggregation was observed with molar ratios as low as 1:50 of HTB1$_{M3}$:SOD1$_{G93A}$, and complete prevention of the formation of ThT-positive SOD1 aggregates was observed at molar ratios as low as 1:10 of HTB1$_{M3}$:SOD1$_{G85R}$ and 1:5 of HTB1$_{M3}$: SOD1$_{G93A}$ (Figure 2A,B). Kinetic studies of SOD1$_{G93A}$ aggregation showed that even when aggregation was not prevented completely, the lag time to the onset of aggregation was extended considerably in the presence of HTB1$_{M3}$, indicating that HTB1$_{M3}$ slowed the seeding process that takes place before the actual formation of ThT-positive fibrils (Figure 2B). Transmission electron microscopy (TEM) was used

FIGURE 1 (A) FACS analysis of binding affinity of isolated HTB1 clones from sorted libraries. Individual HTB1 clones were isolated from the sorted libraries, stained with anti-cMyc antibody to test for expression, and incubated with biotinylated SOD1$_{G85R}$ or SOD1$_{G93A}$ to test for binding to each of the two SOD1 mutants (each mutant was used at two different concentrations). Each of the four segments in each bar represent the mean fluorescence detected for each clone normalized to the maximum fluorescence. The bar graph represents the binding affinity of the different HTB1 clones to 100 nM (blue) or 400 n*M* (red) SOD1$_{G85R}$ or 50 nM (green) or 100 n*M* (purple) SOD1$_{G93A}$. The HTB1 clones selected for purification, namely, HTB1$_{M3}$ and HTB1$_{M4}$, are indicated with brown rectangles. (B,C) PDB structures of HTB1 showing (in brown) the mutation positions that were previously used to generate HTB1$_M$ from HTB1$_{WT}$ and (in red using a stick representation) the positions of newly introduced mutations in HTB1$_{M3}$ (B) and HTB1$_{M4}$ (C)
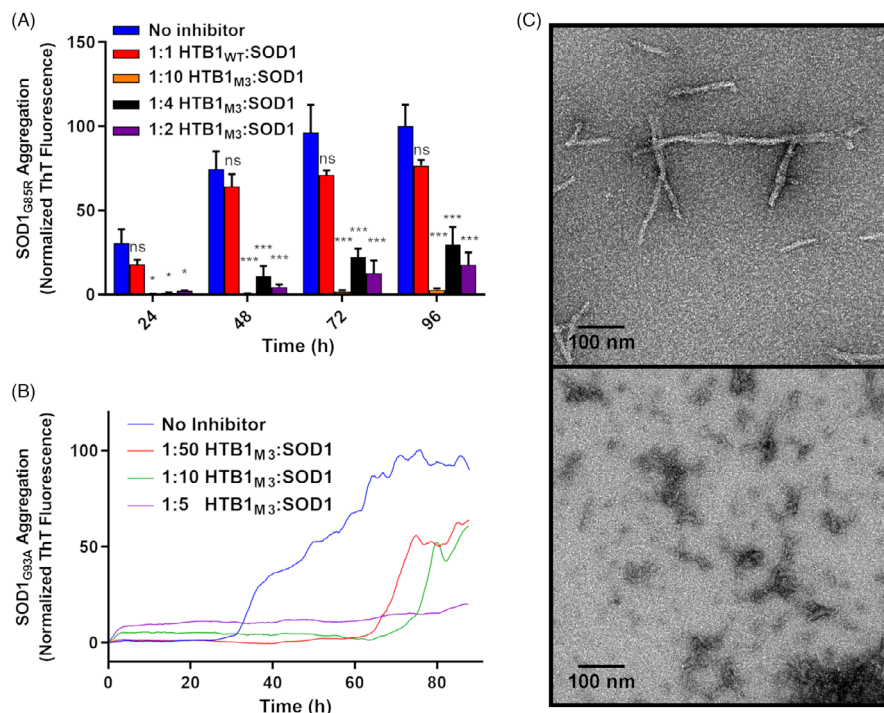
(A)

(B)

(C)
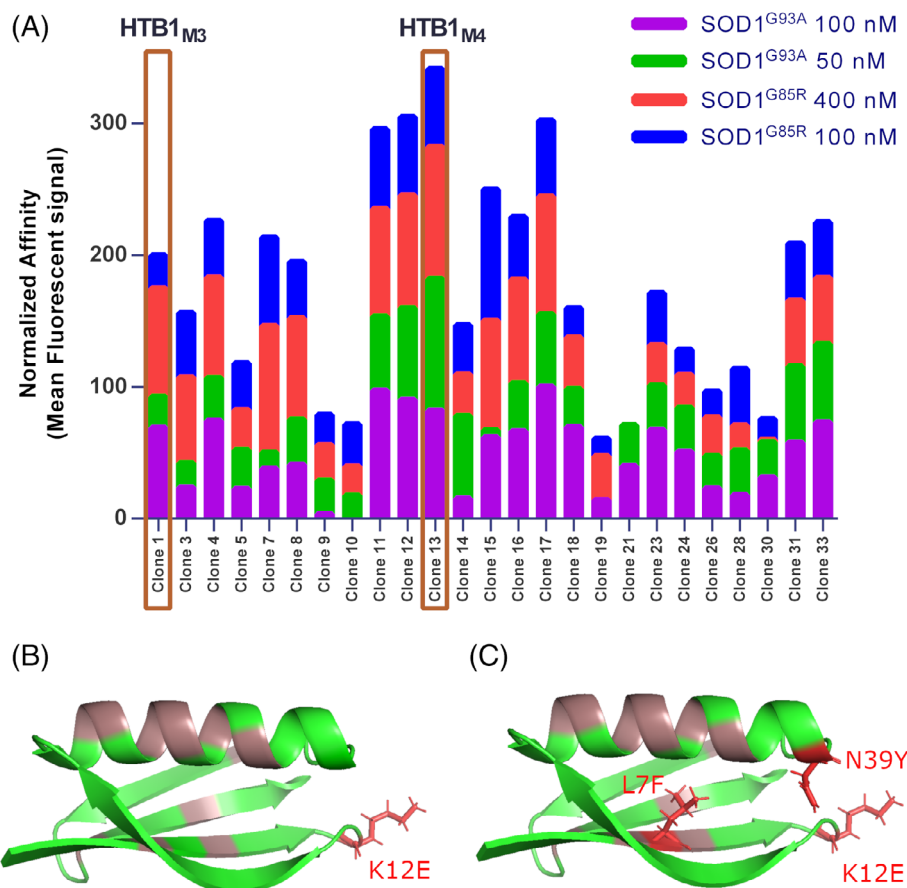
FIGURE 2 HTB1$_{M3}$ inhibits SOD1$_{G85R}$ and SOD1$_{G93A}$ aggregation. SOD1$_{G85R}$ (A) and SOD1$_{G93A}$ (B) were incubated under aggregation-inducing conditions for 4 days in the absence or presence of different concentrations of HTB1$_{M3}$. Aggregation was quantified by monitoring ThT fluorescence either continuously (B) or by end-point measurements (A) using excitation at 445 nm and emission at 485 nm; these results were normalized to the maximum fluorescence detected in each experiment. All experimentally acquired values for A and B are averages of at least three repetitions, with the bars in panel A representing SD. Dunnett's test was used for statistical analysis in panel A to compare each experiment to the untreated control for the same time point. ns—not significant, ***$P < .001$ and *$P < .05$. (C) TEM was used to confirm the presence of fibrillar amyloid aggregates in samples of untreated SOD1$_{G85R}$ (top) and SOD1$_{G85R}$ treated with 25 μM HTB1$_{M3}$ (bottom), in which fibrillar amyloid aggregates were absent but amorphous protein aggregates were detected. SOD1 concentration in all samples was 50 μM [Color figure can be viewed at wileyonlinelibrary.com]

to verify the existence of SOD1$_{G85R}$ amyloid-like fibrils in untreated samples and the absence of amyloid fibrils in samples treated with HTB1$_{M3}$. In the presence of HTB1$_{M3}$, amorphous protein aggregates were observed, but the structured fibrils that are characteristic of amyloid aggregation were not found (Figure 2C). These findings are consistent with the ThT results showing that HTB1$_{M3}$ inhibited the formation of fully formed, filamentous fibrils. They also show that SOD1 did not remain in a dimeric (or monomeric) form in the presence of HTB1$_{M3}$, but instead formed amorphous unstructured aggregates (which are not ThT responsive).

3.3 | SOD1 forms non-ThT responsive oligomers when treated with HTB1$_{M3}$

To better define the oligomeric species that are formed upon treatment of SOD1 with HTB1$_{M3}$, we used the anti-amyloid oligomers (A11) antibody, which has been shown to recognize amyloid prefibrillar oligomer species but not mature amyloid fibrils or monomers.[30-32] The formation of oligomers of SOD1$_{G93A}$ was followed for 96 hours under aggregation-inducing conditions (Figure 3). As expected, in the absence of HTB1$_{M3}$, SOD1$_{G93A}$ first exhibited a seeding phase, lasting 24 to 48 hours, in which the signal from A11 increased as the protein assembled into oligomers (Figure 3). As is evident from the ThT experiment described above, the seeding phase of SOD1$_{G93A}$ is completed after 48 hours, and the oligomers then assemble into fully formed amyloid fibrils. Accordingly, after 48 hours the signal from A11 antibody disappeared completely. In the presence of HTB1$_{M3}$, the initial oligomerization process of SOD1$_{G93A}$ was not affected, as was indicated by a

strong signal from the A11 antibody after 24 and 48 hours, similarly to the sample without HTB1$_{M3}$. However, in the presence of 20 μM or 50 μM HTB1$_{M3}$, SOD1$_{G93A}$ fibrillization was delayed to 72 hours and 96 hours, respectively, and prefibrillar oligomers were detected by A11 antibody throughout the entire 96-hours period of the experiment. Therefore, the presence of HTB1$_{M3}$ (although not affecting the initial oligomerization phase of SOD1 aggregation) delayed the elongation phase in which the oligomers form mature fibrils. Samples of HTB1$_{M3}$ alone, without SOD1$_{G93A}$, showed a negligible reaction with A11 antibody, indicating that the presence of HTB1$_{M3}$ does not affect the A11 signal directly (Figure 3, bottom). These results correlate well with the ThT and TEM results showing that HTB1$_{M3}$ inhibits the formation of mature amyloid fibrils but encourages the formation of A11-responsive SOD1 prefibrillar oligomers.

3.4 | SOD1 oligomers formed in the presence of HTB1$_{M3}$ are nontoxic to NSC-34 cells

Inhibition of SOD1$_{G93A}$ aggregation and the formation of oligomers in the presence of HTB1$_{M3}$ (indicated by the ThT, TEM, and A11 antibody dot blots) gives rise to the question of whether HTB1$_{M3}$ can prevent the toxicity exhibited by misfolded SOD1 aggregates, not only in the fibrillar form, but also in certain oligomeric forms that are toxic to neurons. The ThT and TEM results (described above, Figure 2) showed that HTB1$_{M3}$ directs SOD1 mutants to an oligomerization pathway that leads to the formation of SOD1 oligomers but not to the formation of mature fibrils. We therefore used the NSC-34 motor neuron-like cell line to test the effect of the aggregate-forming
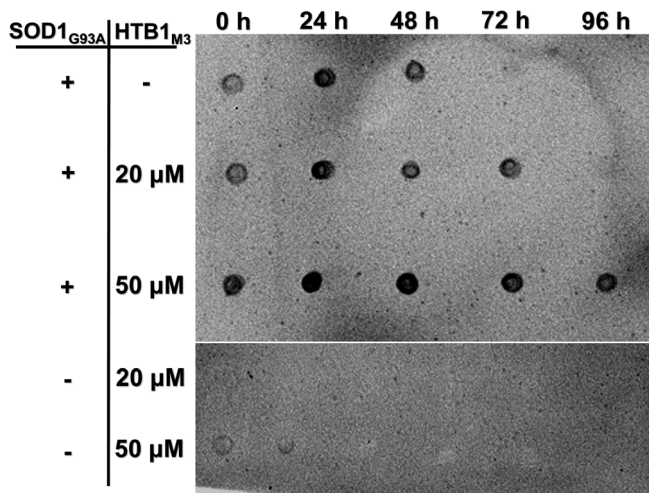
FIGURE 3 SOD1$_{G93A}$ oligomers formed in the presence of HTB1$_{M3}$ do not reassemble into mature amyloid fibrils. Samples taken from aggregation reactions of SOD1$_{G93A}$ were dot-blotted using A11 antibody, which recognizes amyloid prefibrillar oligomer species but not mature amyloid fibrils or monomers. From top to bottom: untreated SOD1$_{G93A}$, with no signal apparent after 72 and 96 hours; SOD1$_{G93A}$ aggregated in the presence of 20 μM HTB1$_{M3}$; SOD1$_{G93A}$ aggregated in the presence of 50 μM HTB1$_{M3}$; 20 μM HTB1$_{M3}$; and 50 μM HTB1$_{M3}$. In this experiment, SOD1$_{G93A}$ was used at a concentration of 6 μM monomer-equivalent. Dot blots were conducted in triplicate, and a representative blot is shown for each experimental condition. For each experiment, 2 μL from each aggregation sample were used for the blotting. Different time points represent samples taken from the same tube, in which SOD1 was allowed to continuously aggregate for 96 hours at 37°C with 600 RPM orbital shaking

SOD1$_{G85R}$ and SOD1$_{G93A}$ on cell viability, in the presence or absence of HTB1$_{M3}$, that is, to determine whether the mutant SOD1 oligomers were toxic or nontoxic. To this end, SOD1$_{G93A}$ or SOD1$_{G85R}$ aggregates were prepared by incubating the mutant proteins for 48 hours under the same aggregation-inducing conditions as were used for the ThT and A11 antibody experiments described above. Prior to exposure to the NSC-34 cells, the aggregates were dialyzed in PBS overnight to remove the TCEP and EDTA used in aggregation, since these compounds are toxic to the cells. As expected, treating the cells with 6 μM monomer-equivalent of SOD1$_{G93A}$ or SOD1$_{G85R}$ for 16 hours led to a reduction of 15% and 10% in cell viability, respectively. While an additional small reduction in viability was obtained upon exposing the cells to SOD1 mutants that had aggregated in the presence of 1 μM HTB1$_{M3}$, cell viability was not impaired when the neuronal cells were treated with SOD1$_{G93A}$ or SOD1$_{G85R}$ aggregates that had been exposed to 5 μM or 10 μM HTB1$_{M3}$ (Figure 4A,B). Thus, to assess whether HTB1$_{M3}$ protects cells from toxicity by directly preventing aggregation, as was indicated by the ThT experiments, or by neutralizing the toxicity of aggregates, we measured the ThT fluorescence signal of SOD1 aggregates prior to exposure to the cells. We found a high correlation (ie, $R = -0.9570 \pm 0.0354$) between the ThT signal of samples and the viability of the cells exposed to those samples, indicating that HTB1$_{M3}$ prevents toxicity by modulating/altering the aggregation

pathway and not by affecting the interaction of preformed aggregates with the cells upon exposure of the cell cultures to the aggregates (Figure 4C).

3.5 | Extracellular HTB1$_{M3}$ prevents SOD1$_{G93A}$ penetration into neuronal cells

The prion-like nature of misfolded SOD1 allows it to propagate from cell to cell and seed aggregation in infected cells, thereby spreading the toxic species of SOD1 in the central nervous system. An important component of this process is the internalization of extracellular misfolded SOD1 into neurons—a highly efficient process that takes place when neurons are exposed to misfolded SOD1, SOD1 oligomers or SOD1 mature amyloid fibrils. To assess the effect of HTB1$_{M3}$ on the internalization process of SOD1, we used fluorescently labeled SOD1$_{G93A}$—either aggregated in-vitro prior to exposure to the cells or in the native nonaggregated form. When incubated with the cells for 16 hours in the absence of HTB1$_{M3}$, both aggregated and nonaggregated SOD1$_{G93A}$ penetrated into NSC-34 cells with high efficiency. In the presence of HTB1$_{M3}$, the amount of SOD1 that penetrated the cells was markedly reduced in an HTB1$_{M3}$-dose-dependent manner (Figure 5A). The results of FACS analysis of the cells were verified by confocal microscopy, using both fluorescently labeled SOD1$_{G93A}$ and fluorescently labeled HTB1$_{M3}$. Cells incubated with 0.5 μM SOD1$_{G93A}$ in the presence of 0.64 μM HTB1$_{M3}$ internalized a far smaller amount of SOD1 aggregates (Figure 5C) than cells incubated with SOD1 alone (Figure 5B). These findings show that HTB1$_{M3}$ counters SOD1$_{G93A}$ toxicity both by preventing the formation of extracellular toxic SOD1 oligomers and fibrils and also by preventing the penetration of preformed toxic species into neurons.

4 | DISCUSSION AND CONCLUSION

Mutations in the *SOD1* gene, such as G85R and G93A, that render the protein prone to misfolding and aggregation are the second most prevalent cause of fALS, being found in 20% of fALS cases.[5,33] The mechanism by which SOD1$_{G93A}$ and SOD1$_{G85R}$ exert their toxic effect is still unknown, but a clear association has been shown between misfolding and aggregation of SOD1$_{G93A}$ and SOD1$_{G85R}$ and neuronal dysfunction and death in ALS.[34-37] Some therapeutic approaches to prevent or attenuate ALS progression have therefore centered on interfering with this misfolding and aggregation of SOD1 mutants, and numerous small molecules, peptide mimetics and antibodies that target misfolded SOD1 and inhibit its aggregation have been developed. These include: various small molecules that were predicted to bind at the SOD1 dimer interface and thereby to inhibit SOD1$_{G85R}$ and SOD1$_{G93A}$ aggregation[38]; macrophage migration inhibitory factor, which has been shown to inhibit misfolding and aggregation of SOD1$_{G93A}$ and SOD1$_{G85R}$[39]; and the small heat-shock proteins αB-crystallin and Hsp27, which suppress SOD1$_{G93A}$ aggregation.[40] Nevertheless, despite intensive research, there is still no drug targeting SOD1 or the SOD1 aggregation process that
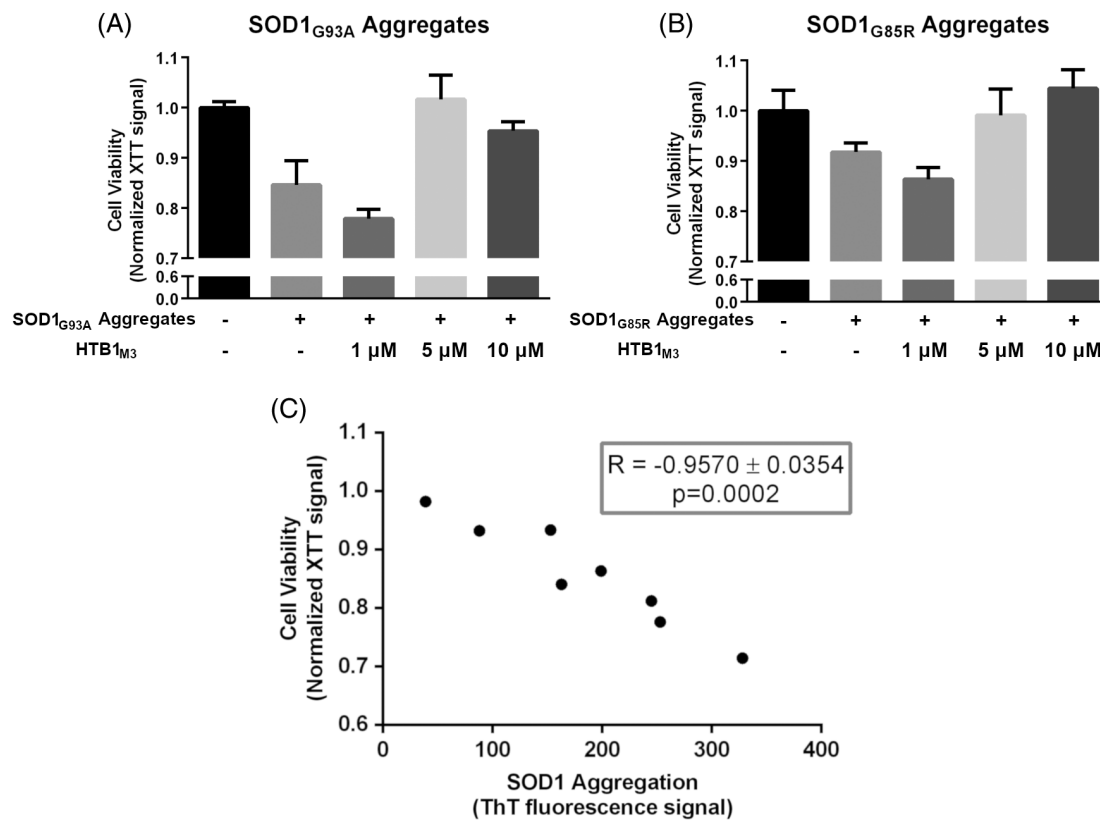
FIGURE 4 HTB1$_{M3}$ reduces neurotoxicity of SOD1 aggregates in NSC-34 cell culture. The viability of NSC-34 cell cultures was determined after exposure of the cells to 6 μM monomer-equivalent of SOD1 that had been allowed to aggregate in the presence or absence of HTB1$_{M3}$. Cell cultures were exposed to the aggregates overnight, after dialysis of the aggregates to remove residual TCEP and EDTA from the solution. Cell viability from three independent experiments is presented for (A) SOD1$_{G93A}$ and (B) SOD1$_{G85R}$ normalized to the untreated sample. (C) A plot of the correlation between the ThT signal for SOD1 aggregation levels with the toxicity of the aggregates to the cells. Data was pooled from all toxicity experiments, including for both SOD1$_{G93A}$ and SOD1$_{G85R}$ aggregates and various concentrations of HTB1$_{M3}$. The Pearson correlation with 95% confidence intervals is $R = -0.9570 \pm 0.0354$, with a two-tailed P-value of .0002

has been sufficiently successful in clinical trials to be approved by the FDA. Furthermore, recent evidence suggests that preventing the formation of amyloid fibrils alone may not have a beneficial therapeutic effect and may even have the opposite effect of increasing the concentration of SOD1 toxic oligomeric species by preventing the formation of the less toxic mature fibrils.[41]

One of the factors impeding progress in the development of therapeutics targeting ALS is the lack of reliable biophysical methods to detect toxic SOD1 species. ThT fluorescence is still the most widely used method to detect SOD1 aggregation, but this method cannot distinguish toxic from nontoxic SOD1 aggregates. Furthermore, while certain oligomeric species, such as the SOD1 trimer have been shown to be toxic in vitro,[42] the methods used for detection of these oligomeric species are not suitable for in-vivo studies, precluding the direct detection of these oligomeric species in vivo. A variety of antibodies, among them the A11 oligomer-specific antibody, have been suggested as universal antibodies for detecting toxic amyloid species,[31,32] but these antibodies do not always reliably distinguish between toxic and nontoxic forms.[43] Indeed, we showed here that while A11 recognized SOD1 oligomers but not SOD1 monomers or mature fibrils, it was unable to distinguish between the nontoxic and toxic SOD1$_{G93A}$

oligomeric species that were formed in the presence or absence of HTB1$_{M3}$ (Figures 3 and 4). In addition, the findings of our experiments with this antibody did not enable us to establish a correlation between toxicity and aggregation.

In light of the above, a potentially applicable innovative finding of this study was the strong correlation between ThT responsiveness and the toxicity of SOD1 aggregating in the presence of HTB1$_{M3}$. We therefore propose that ThT responsiveness can be used as an indicator of toxicity in certain cases, such as when SOD1 is treated with HTB1$_{M3}$, even though ThT is generally considered not responsive to oligomers and therefore unable to directly detect toxic species. Our findings show that HTB1$_{M3}$ inhibits the formation of ThT-positive mature amyloid fibrils by extending the lag time of their formation kinetics and by reducing the end-stage ThT signal, which correlates with the amount of mature amyloid fibrils (Figure 2). Both TEM (Figure 2C) and A11 antibody dot blot (Figure 3) results reveal that HTB1$_{M3}$ does not prevent the formation of oligomers, but instead encourages the formation of oligomers that do not reorganize into mature amyloid fibrils (off-pathway oligomers). Most importantly, we show here for the first time that the oligomers formed in the presence of HTB1$_{M3}$ are not toxic to the NSC-34 neuronal cell line (Figure 4A,B)
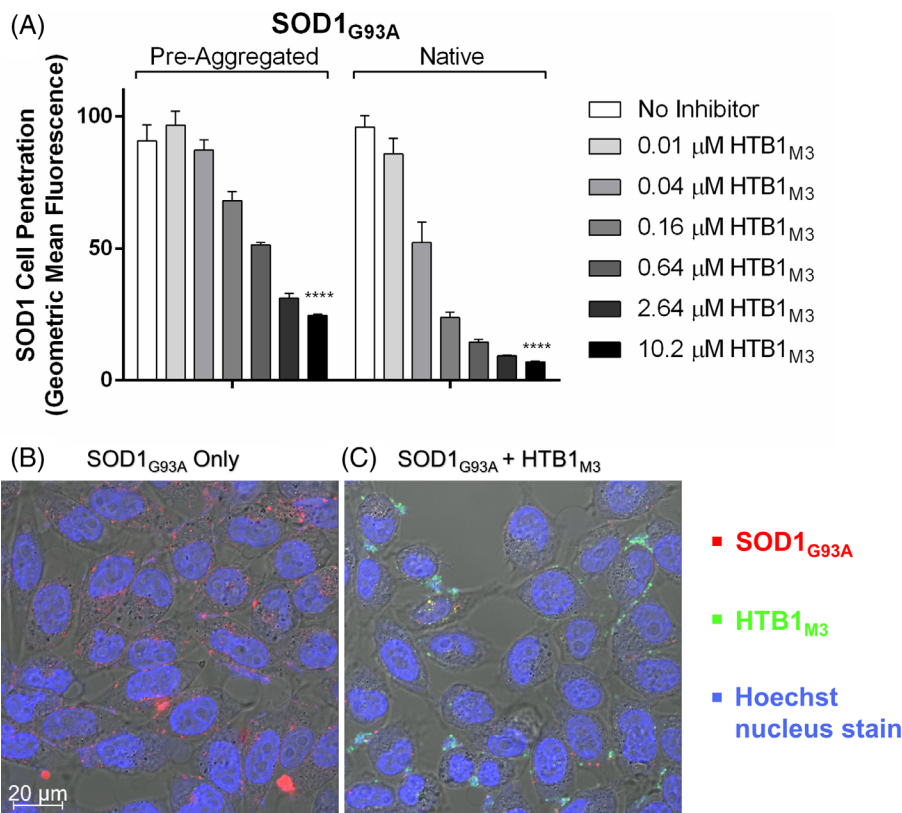
FIGURE 5 HTB1$_{M3}$ blocks the penetration of SOD1$_{G93A}$ into NSC-34 cells. AlexaFluor-647 conjugated SOD1$_{G93A}$ (0.05 μM) was added to the NSC-34 cell culture medium in the presence or absence of HTB1$_{M3}$. After 16 hours, cells were treated with trypsin and washed three times with PBS prior to measuring fluorescence by FACS. Each sample (containing 15 000 cells) was analyzed, and geometric mean fluorescence was calculated and plotted. (A) Left-hand and right-hand panels show mean fluorescence for SOD1$_{G93A}$ preaggregated for 48 hours under aggregation-inducing conditions and native SOD1$_{G93A}$, without preaggregation, respectively. Statistical analysis of three experiments was performed using Bonferroni's multiple comparison test. **** indicates $P < .0001$. (B,C) Confocal images of untreated cells (B) and cells treated with 0.64 μM HTB1$_{M3}$ (C), both in the presence of 0.5 μM SOD1$_{G93A}$. Red, green, and blue indicate SOD1$_{G93A}$ labeled with Alexafluor-647, HTB1$_{M3}$ labeled with Dylight-488, and nuclei stained with Hoechst nucleus stain, respectively. Cells were washed with cell culture medium to remove extracellular proteins and immediately imaged using a ×63 magnification lens. All results represent pooled data from at least three independent experiments [Color figure can be viewed at wileyonlinelibrary.com]

and that there is a strong correlation between the ThT signal, an indicator of mature amyloid fibrils and of the toxicity of the SOD1 species formed in the presence of HTB1$_{M3}$ (Figure 4C). Such a correlation was not observed in the absence of HTB1$_{M3}$ where SOD1 aggregates to fully formed ThT-positive fibrils, and therefore in this case the easy-to-perform ThT assay cannot be used as a measure of toxicity.[41,43] Therefore, we conclude that monitoring ThT fluorescence provides a simple and reliable way to monitor the inhibition of SOD1 toxicity by HTB1$_{M3}$ and propose that this simple assay can be applied in the future to monitoring yet-to-be-developed inhibitors.

A different aspect of our work relates to the spatiotemporal progression of ALS, with neuronal damage being first manifested at focal points, but quickly spreading throughout the brain stem, motor cortex, and spinal cord. This spread of neuronal damage has been linked to misfolded SOD1 acting in a prion-like manner, namely, SOD1 secreted by inflicted cells infects neighboring neurons and seeds SOD1 misfolding and aggregation in naïve neuronal cells.[11,13,20,44] For example, the in-vitro study of Munch et al showed that once misfolded SOD1 penetrates neurons, it seeds the misfolding and aggregation of SOD1

inside the infected neurons and is also secreted back into the medium to infect more neurons.[20] The presence of misfolded SOD1 in the CSF of both sporadic ALS and fALS patients implies that this prion-like process could be an important factor in the spread of the disease throughout the central nervous system and that targeting this process could delay or even completely halt the progression of the disease. In accordance with these findings, we found that both the aggregated and native-misfolded forms of SOD1 penetrate NSC-34 cells with very high efficiency. Importantly, we showed for the first time that when HTB1$_{M3}$ is present in the culture medium it can inhibit the propagation of SOD1 by interfering directly in the internalization process of SOD1 from the culture medium into the cells in a dose-dependent manner (Figure 5). HTB1$_{M3}$ could therefore be used as an agent that not only drives SOD1 to form nontoxic oligomers but also prevents the internalization of toxic SOD1 species inside neurons, where they inflict the most damage. Since it has been proposed that the mechanism for SOD1 internalization is macropinocytosis,[45] and since HTB1$_{M3}$ completely suppresses the internalization process of SOD1, further study is required to address the role of macropinocytosis

in SOD1 internalization and the question of whether HTB1$_{M3}$ inhibits this internalization directly or indirectly by interaction with SOD1.

In summary, the study establishes proof-of-principle for a novel library screening approach that will be widely applicable for evolving affinity and specificity in tandem with aggregation-inhibiting functionality for diverse protein scaffolds. In addition, it identifies a promising inhibitor of SOD1^{G93A} and SOD1^{G85R} as a starting point for the development of an anti-amyloid protein therapy for fALS. The next stage of our study will therefore be to evaluate the therapeutic potential of HTB1$_{M3}$. To this end, we will use AAV9 as a carrier to deliver HTB1$_{M3}$ to the central nervous system, since intravenously injected AAV9 has been shown to successfully cross the blood-brain barrier (BBB) and target neurons and astrocytes in the brain.[46,47] This gene-therapy oriented method of delivery circumvents for stably expressing HTB1$_{M3}$ in neurons allows for a controlled release mechanism, which may lead to more stable levels of HTB1$_{M3}$ over longer periods. We propose that HTB1$_{M3}$ may be suitable for combination with the AAV9 delivery system in order to prevent the formation of toxic SOD1 aggregates and their propagation in vivo.

ACKNOWLEDGMENTS

CONFLICT OF INTEREST

The authors declare that they have no conflict of interest with respect to publication of this article.

ORCID

Niv Papo https://orcid.org/0000-0002-7056-2418

REFERENCES

1. Caughey B, Lansbury PT. Protofibrils, pores, fibrils, and neurodegeneration: separating the responsible protein aggregates from the innocent bystanders. *Annu Rev Neurosci*. 2003;26(1):267-298.

2. Kiernan MC, Vucic S, Cheah BC, et al. Amyotrophic lateral sclerosis. *The Lancet*. 2011;377(9769):942-955.

3. Gurney ME, Pu H, Chiu AY, et al. Motor neuron degeneration in mice that express a human Cu, Zn superoxide dismutase mutation. *Science*. 1994;264(5166):1772-1775.

4. Ajroud-Driss S, Siddique T. Sporadic and hereditary amyotrophic lateral sclerosis (ALS). *Biochimica et Biophysica Acta - Molecular Basis Dis*. 2015;1852(4):679-684.

5. Wroe R, Wai-Ling Butler A, Andersen PM, Powell JF, Al-Chalabi A. ALSOD: the amyotrophic lateral sclerosis online database. *Amyotroph Lateral Scler*. 2008;9(4):249-250.

6. Graffmo KS, Forsberg K, Bergh J, et al. Expression of wild-type human superoxide dismutase-1 in mice causes amyotrophic lateral sclerosis. *Hum Mol Genet*. 2012;22(1):51-60.

7. Lourenco GF, Janitz M, Huang Y, Halliday GM. Long noncoding RNAs in TDP-43 and FUS/TLS-related frontotemporal lobar degeneration (FTLD). *Neurobiol Dis*. 2015;82:445-454.

8. Palomo GM, Manfredi G. Exploring new pathways of neurodegeneration in ALS: the role of mitochondria quality control. *Brain Res*. 2015;1607:36-46.

9. Nishitoh H, Kadowaki H, Nagai A, et al. ALS-linked mutant SOD1 induces ER stress- and ASK1-dependent motor neuron death by targeting Derlin-1. *Genes Dev*. 2008;22(11):1451-1464.

10. Haase G, Rabouille C. Golgi fragmentation in ALS motor neurons. New mechanisms targeting microtubules, tethers, and transport vesicles. *Front Neurosci*. 2015;9:448.

11. Polymenidou M, Cleveland DW. The seeds of neurodegeneration: prion-like spreading in ALS. *Cell*. 2011;147(3):498-508.

12. Nonaka T, Masuda-Suzukake M, Arai T, et al. Prion-like properties of pathological TDP-43 aggregates from diseased brains. *Cell Rep*. 2013;4(1):124-134.

13. Münch C, Bertolotti A. Self-propagation and transmission of misfolded mutant SOD1: prion or prion-like phenomenon? *Cell Cycle*. 2011;10(11):1711.

14. Corsaro A, Thellung S, Villa V, Nizzari M, Florio T. Role of prion protein aggregation in neurotoxicity. *Int J Mol Sci*. 2012;13(7):8648-8669.

15. Sekiguchi T, Kanouchi T, Shibuya K, et al. Spreading of amyotrophic lateral sclerosis lesions-multifocal hits and local propagation? *J Neurol Neurosurg Psychiatry*. 2014;85(1):85-91.

16. Ravits JM, La Spada AR. Als motor phenotype heterogeneity, focality, and spread: deconstructing motor neuron degenerationsymbol. *Neurology*. 2009;73(10):805-811.

17. Jacobsson J, Jonsson P a, Andersen PM, Forsgren L, Marklund SL. Superoxide dismutase in CSF from amyotrophic lateral sclerosis patients with and without CuZn-superoxide dismutase mutations. *Brain*. 2001;124(7):1461-1466.

18. Urushitani M, Sik A, Sakurai T, Nukina N, Takahashi R, Julien JP. Chromogranin-mediated secretion of mutant superoxide dismutase proteins linked to amyotrophic lateral sclerosis. *Nat Neurosci*. 2006;9(1):108-118.

19. Gomes C, Keller S, Altevogt P, Costa J. Evidence for secretion of cu,Zn superoxide dismutase via exosomes from a cell model of amyotrophic lateral sclerosis. *Neurosci Lett*. 2007;428(1):43-46.

20. Munch C, O'Brien J, Bertolotti A. Prion-like propagation of mutant superoxide dismutase-1 misfolding in neuronal cells. *Proc Natl Acad Sci*. 2011;108(9):3548-3553.

21. Takeuchi S, Fujiwara N, Ido A, et al. Induction of protective immunity by vaccination with wild-type apo superoxide dismutase 1 in mutant SOD1 transgenic mice. *J Neuropathol Exp Neurol*. 2010;69(10):1044-1056.

22. Gros-Louis F, Soucy G, Larivière R, Julien JP. Intracerebroventricular infusion of monoclonal antibody or its derived fab fragment against misfolded forms of SOD1 mutant delays mortality in a mouse model of ALS. *J Neurochem*. 2010;113(5):1188-1199.

23. Liu H, Tjostheim S, Dasilva K, et al. Targeting of monomer/Misfolded SOD1 as a therapeutic strategy for amyotrophic lateral sclerosis. *Neurobiol Dis*. 2012;32(26):8791-8799.

24. Foust KD, Salazar DL, Likhite S, et al. Therapeutic AAV9-mediated suppression of mutant SOD1 slows disease progression and extends survival in models of inherited ALS. *Mol Ther*. 2013;21(12):2148-2159.

25. Lu H, Le W, Xie YY, Wang XP. Current therapy of drugs in amyotrophic lateral sclerosis. *Curr Neuropharmacol*. 2016;14(4):314-321.

26. Petrov D, Mansfield C, Moussy A, Hermine O. ALS clinical trials review: 20 years of failure. Are we any closer to registering a new treatment? *Front Aging Neurosci*. 2017;9:68.

27. Smith TJ, Stains CI, Meyer SC, Ghosh I. Inhibition of β-amyloid fibrillization by directed evolution of a β-sheet presenting miniature protein. *J Am Chem Soc*. 2006;128(45):14456-14457.

28. Banerjee V, Oren O, Ben-Zeev E, Taube R, Engel S, Papo N. A computational-combinatorial approach identifies a protein inhibitor of superoxide dismutase 1 misfolding, aggregation, and cytotoxicity. *J Biol Chem*. 2017;292(38):15777-15788.

29. Chen TS, Palacios H, Keating AE. Structure-based redesign of the binding specificity of anti-apoptotic Bcl-xL. *J Mol Biol*. 2013;425(1):171-185.

30. Kayed R, Head E, Sarsoza F, et al. Fibril specific, conformation dependent antibodies recognize a generic epitope common to amyloid fibrils and fibrillar oligomers that is absent in prefibrillar oligomers. *Mol Neurodegen*. 2007;2(1):18.

31. Hu Y, Su B, Kim CS, et al. A strategy for designing a peptide probe for detection of β-amyloid oligomers. *Chembiochem*. 2010;11(17):2409-2418.

32. Kayed R, Head E, Thompson JL, et al. Common structure of soluble amyloid oligomers implies common mechanism of pathogenesis. *Science*. 2003;300(5618):486-489.

33. Leblond CS, Kaneb HM, Dion PA, Rouleau GA. Dissection of genetic factors associated with amyotrophic lateral sclerosis. *Exp Neurol*. 2014;262(Part B):91-101.

34. Sheng Y, Chattopadhyay M, Whitelegge J, Valentine JS. SOD1 aggregation and ALS: role of metallation states and disulfide status. *Curr Top Med Chem*. 2012;12(22):2560-2572.

35. Magrané J, Cortez C, Gan WB, Manfredi G. Abnormal mitochondrial transport and morphology are common pathological denominators in SOD1 and TDP43 ALS mouse models. *Hum Mol Genet*. 2013;23(6):1413-1424.

36. Furukawa, Y. Protein aggregates in pathological inclusions of amyotrophic lateral sclerosis. Amyotrophic Lateral Sclerosis. *Neurol Res Int*. 2012;2012:323261.

37. Abu-Hamad S, Kahn J, Leyton-Jaimes MF, Rosenblatt J, Israelson A. Misfolded SOD1 accumulation and mitochondrial association contribute to the selective vulnerability of motor neurons in familial ALS: correlation to human disease. *ACS Chem Nerosci*. 2017;8(10):2225-2234.

38. Ray SS, Nowak RJ, Brown RH, Lansbury PT. Small-molecule-mediated stabilization of familial amyotrophic lateral sclerosis-linked superoxide dismutase mutants against unfolding and aggregation. *Proc Natl Acad Sci U S A*. 2005;102(10):3639-3644.

39. Shvil N, Banerjee V, Zoltsman G, et al. MIF inhibits the formation and toxicity of misfolded SOD1 amyloid aggregates: implications for familial ALS article. *Cell Death and Disease*. 2018;9(2):107.

40. Yerbury JJ, Gower D, Vanags L, Roberts K, Lee JA, Ecroyd H. The small heat shock proteins αb-crystallin and Hsp27 suppress SOD1 aggregation in vitro. *Cell Stress and Chaperones*. 2013;18(2):251-257.

41. Zhu C, Beck MV, Griffith JD, Deshmukh M, Dokholyan NV. Large SOD1 aggregates, unlike trimeric SOD1, do not impact cell viability in a model of amyotrophic lateral sclerosis. *Proc Natl Acad Sci*. 2018;115(18):201800187.

42. Proctor EA, Fee L, Tao Y, et al. Nonnative SOD1 trimer is toxic to motor neurons in a model of amyotrophic lateral sclerosis. *Proc Natl Acad Sci*. 2016;113(3):614-619.

43. Chiti F, Dobson CM. Protein Misfolding, amyloid formation, and human disease: a summary of Progress over the last decade. *Annu Rev Biochem*. 2017;86(1):27-68.

44. Lee S, Kim H-J. Prion-like mechanism in amyotrophic lateral sclerosis: are protein aggregates the key? *Exp Neurobiol*. 2015;24(1):1-7.

45. Zeineddine R, Pundavela JF, Corcoran L, et al. SOD1 protein aggregates stimulate macropinocytosis in neurons to facilitate their propagation. *Mol Neurodegen*. 2015;10(1):57.

46. Duque S, Joussemet B, Riviere C, et al. Intravenous administration of self-complementary AAV9 enables transgene delivery to adult motor neurons. *Mol Ther*. 2009;17(7):1187-1196.

47. Foust KD, Nurre E, Montgomery CL, Hernandez A, Chan CM, Kaspar BK. Intravascular AAV9 preferentially targets neonatal neurons and adult astrocytes. *Nat Biotechnol*. 2008;27(1):59-65.

SUPPORTING INFORMATION

Additional supporting information may be found online in the Supporting Information section at the end of this article.